Macromolecules

ARTICLE

pubs.acs.org/Macromolecules

ε-Caprolactone-Based Macromonomers Suitable for Biodegradable Nanoparticles Synthesis through Free Radical Polymerization

Raffaele Ferrari,[†] Yingchuan Yu,[‡] Massimo Morbidelli,[‡] Robin A. Hutchinson,[§] and Davide Moscatelli*[,†]

[†]Dipartimento di Chimica, Materiali e Ingegneria Chimica "Giulio Natta", Politecnico di Milano, 20131, Milano, Italy

[‡]Institute for Chemical and Bioengineering, Department of Chemistry and Applied Biosciences, ETH Zurich, 8093, Zurich, Switzerland

[§]Department of Chemical Engineering, Dupuis Hall, Queen's University, Kingston, Ontario K7L 3N6, Canada

Supporting Information

ABSTRACT: New ε-caprolactone (CL)-based materials were synthesized. Bulk ring-opening polymerization of ε-caprolactone with 2-hydroxyethyl methacrylate (HEMA) as cocatalyst was carried out to produce various macromonomers composed of HEMA functionalized with 1−10 CL units. All of the HEMA-CL macromonomers have been characterized by size exclusion chromatography (SEC) and ^{1}H NMR. For SEC analysis universal calibration was applied, and Mark−Houwink parameters for poly(HEMA-*g*-CL_3) were obtained. Macromonomers with different CL chain length were polymerized through free radical polymerization, in both batch and semibatch emulsion polymerization to produce CL-based nanoparticles (NPs) with narrow particle size distribution. Various reactions parameters were investigated, namely the type of the emulsifier, the feeding conditions, and the macromonomer chain length. Finally, a simple and qualitative degradation study of selected samples was carried out in order to verify the degradability of these CL-based NPs.

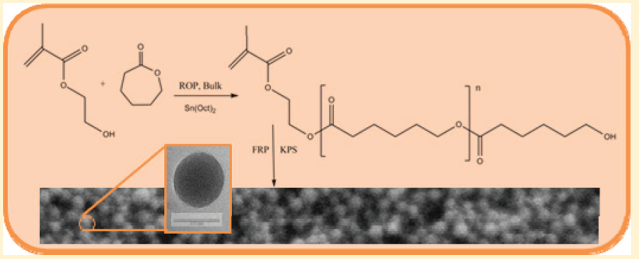

1. INTRODUCTION

Polyesters and copolyesters such as poly(lactic acid) (PLA), poly(lactic-*co*-glycolic acid) (PLGA), and poly(ε-caprolactone) (PCL) are gaining an increasing importance in material science because of their biocompatibility and biodegradability.[1,2] Polymers with high molecular weight can be easily produced in large scale through ring-opening polymerization (ROP) of respective cyclic esters.[3,4] These polyesters find many applications in the tissue engineering field,[5] as sutures,[6] and as adhesion barriers.[7] Moreover, these compounds can be regarded as promising polymers for drug delivery applications,[1,8,9] in particular for synthesis of nanoparticles (NPs), because of their nontoxicity, low cost, and biocompatibility.[10] Compared to other biodegradable polymers, PCL is the most resistant to chemical hydrolysis because of its high hydrophobicity and, as a consequence, is usually employed when a long biodegradability time is required.[11,12] Moreover, for delivery applications, NPs made of PCL show good encapsulation efficiency for a wide range of drugs.[13−15] Nowadays, PCL NPs are prepared in many different ways, mainly by nanoprecipitation,[16,17] solvent displacement,[18,19] and solvent evaporation[20] of the pure PCL or acrylates functionalized with PCL.[21] All of these methods involve either medium or high molecular weight polymers produced through bulk ROP that are mixed with solvent, water, and, eventually, emulsifiers. Through these processes it is possible to obtain stable NPs latexes with suitable sizes for drug delivery. However, these procedures require the use of an organic solvent which must be completely removed from the final solution for all the biological and medical purposes. Moreover, NPs obtained with these methods usually show a relative high polydispersity index whereas a narrow particle size distribution is preferable for drug delivery applications. An additional drawback is that it is quite difficult to obtain a good reproducibility of the final NPs features using these physical procedures. In this paper we report a new approach to avoid these difficulties while producing CL-based NPs.

The procedure adopted to synthesize CL-based NPs involves two steps: the synthesis of new macromonomers based on ε-caprolactone functionalized with a vinyl end group and their subsequent polymerization through FRP in order to obtain NPs.[22] Macromonomers were synthesized through ROP which is a controlled polymerization process. In order to avoid transesterification, a process that leads to a deviation from the controllable behavior of ROP, the reaction is usually stopped before complete conversion is reached. Typically this reaction, which involves a catalyst (tin octoate) and which is initiated by a cocatalyst bearing a hydroxyl group, is used to obtain high molecular weight (MW) polyesters. The final product has a distribution of chain lengths that can be characterized by an average number of CL units added. The cocatalyst plays a strong role, allowing the opening of the lactone ring, thus initiating the growth of the polymer chain,[23,24] since the ROP is a controlled process the MW is expected to be equal to the ratio between ε-caprolactone and alcohol moles. Usually 1-dodecanol

Received: August 29, 2011
Revised: October 17, 2011
Published: November 10, 2011

Scheme 1. Production Route of Poly(HEMA-*g*-CL$_k$) NPs

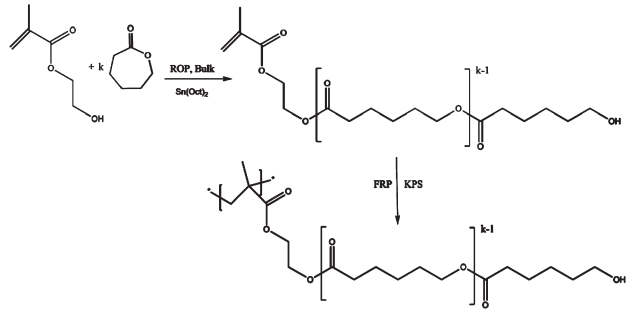

or other high boiling point alcohols are used as cocatalysts in order to reach a good control of the final polymer MW.[25] In this work CL-based polymers with short chain length, between 1 and 10 CL units, were obtained using 2-hydroxyethyl methacrylate (HEMA) as cocatalyst. This hydroxyl bearing species has also a vinyl group that can be preserved by ROP and used for further reaction, in particular in FRP. Note that both the cocatalyst and catalyst are approved by the food and drug administration (FDA) for human use.

The second step of the process is the FRP of these short-chain macromonomers to produce polymer chains consisting of HEMA units, each grafted with k CL units (poly(HEMA-*g*-CL$_k$)). Since emulsion FRP is a well-established process,[26] it is relatively easy to tune the characteristics of the final NPs by changing process parameters such as the amount of emulsifier, the reaction temperature, and the feeding mode.[27,28] Emulsion FRP also ensures the final biocompatibility of the NPs suspensions; in fact, the reaction is carried out in water without using any solvent and adopting a FDA approved emulsifier such as Tween80. Obviously, a more effective surfactant such as SDS can be also used and then substituted with an FDA approved one. As a result, this technique permits the synthesis of polymer biodegradable NPs with all the advantages of an emulsion FRP process: narrow polydispersity index, easy control of the final particle size by changing process parameters, and the absence of any organic solvent used.

Polyesters such as PCL and other CL-based materials degrade with an erosion mechanism as reported in the literature.[29] The polymer matrix size discriminates the possible degradation processes, namely the bulk and surface erosion. For polyesters, such as PCL, a bulk erosion process can be assumed for polymer matrix smaller than 10^{-2} m. As a result, for NPs made of PCL, a bulk erosion process is always expected. In particular, the bulk degradation occurs due to the hydrolysation reactions of ester groups in the PCL chains. The degradation can be observed through the polymer mass loss and the parallel release of 6-hydroxycaproic acid unit and its oligomers, which ultimately degrade into 6-hydroxycaproic acid. Obviously, degradation time is affected by the polymer chain length, with a longer degradation time for high MW polymers compared to for medium or low MW polymers. The strategy developed in this work allows tuning of the degradation time by controlling the number of CL units contained in the macromonomers. The Experimental Section reports the materials used and the synthesis and characterization of macromonomers and NPs. Results are divided in three sections: synthesis of macromonomers, production of NPs, and the degradation study. Finally, the conclusion summarizes the results, focusing on possible future biomedical applications of these materials.

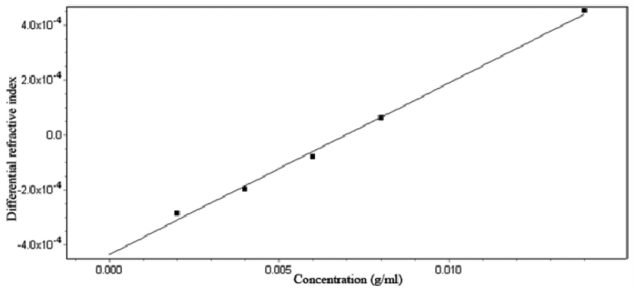

Figure 1. Differential refractive index (dn/dc) values for poly(HEMA-*g*-CL$_3$) in THF at 30 °C.

2. EXPERIMENTAL SECTION

Materials. ε-Caprolactone (Acros, 99% purity), 2-hydroxyethyl methacrylate (Sigma-Aldrich, purity ≥99%), and 2-ethylhexanoic acid tin(II) salt (Sn(Oct)$_2$; Sigma-Aldrich, purity ∼95%) were used without further treatment. For size exclusion chromatography (SEC) analysis THF (Sigma-Aldrich, ≥99.7% purity) was used as eluent. Potassium persulfate (KPS, ≥99% purity), sodium dodecyl sulfate (SDS; Merck, purity ∼90%), Tween80 (Sigma-Aldrich), sodium chloride (Merck, ≥99.5% purity), dichloromethane (Sigma-Aldrich, ≥99.9% purity), and mixed ion-exchange resin (IE; Supelco Analytics) were used as received for NPs production and other treatments.

Macromonomers Synthesis and Characterization. The ROP reaction was carried out without solvent in bulk conditions. CL was first heated up at 130 ± 1 °C in a stirred flask, and the temperature was controlled by an external oil bath. A solution with selected ratio of Sn(Oct)$_2$ and HEMA was then added at the desired molar ratio with respect to monomer in order to control the reaction rate and the final macromonomer average chain length. The reaction was stopped before reaching a complete conversion (above 98% after 90 min) in order to avoid the broadening of the molecular weight distribution (MWD) due to transesterification reactions.[25] All the macromonomers produced were refrigerated at 4 °C for further use. The production route of macromonomers along with their subsequent polymerization is reported in Scheme 1.[22]

Molecular weight distribution of all samples was characterized by size exclusion chromatography (SEC) analysis, using THF as eluent with 0.6 mL/min flow rate and temperature of 35 °C. The instrument (Agilent, 1100 series, Germany) is equipped with two detectors in series (ultraviolet (UV) and differential refractive index (RI)), three PLgel columns (Polymer laboratories Ltd., UK; two with pore sizes of MXC type and one oligopore; 300 mm column length and 7.5 mm i.d.) and a precolumn. Universal calibration was applied, based on polystyrene standards from 580 to 3 250 000 Da (Polymer Laboratories). In order to analyze both polymer and macromonomer molecular weight, poly(HEMA-*g*-CL$_3$) was used to determine Mark−Houwink (MH) parameters on a second SEC setup consisting of a Viscotek 270max separation module and RI, viscosity (IV), and light scattering (low-angle LALS and right-angle RALS) triple detection. A set of two Polyanalytik SuperRes columns with an exclusion limit molecular weight of 20×10^6 g mol^{-1} were used in series at 40 °C, and distilled THF was used as the eluent at a flow rate of 1 mL min^{-1}. The differential index of refraction (dn/dc) of the polymer in THF is required to process data from the triple detector instrument and determine the MH parameters. This measurement was done on a refractometer (Wyatt Optilab DSP) calibrated with sodium chloride, using five poly(HEMA-*g*-CL$_3$) samples of different concentration from 2.0 to 14.0 mg mL^{-1} in THF, injected

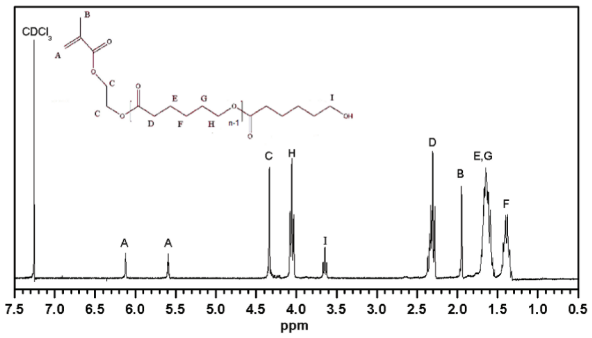

Figure 2. ^{1}H NMR spectra of HEMA-*g*-CL_6 macromonomer.

sequentially to obtain the d*n*/d*c* value, as shown in Figure 1. Once this parameter was determined, MH values were obtained by fitting of the log(viscosity) vs log(MW) plots generated by the triple detector SEC setup. The MH values were used for molecular weight calculation of all the polymers produced with macromonomer up to HEMA-*g*-CL_{10}.

The structure and the composition of macromonomer have been also determined by ^{1}H NMR in $CDCl_3$ using a 500 MHz Ultrashield NMR spectrometer (Bruker, Switzerland). ^{1}H NMR molecular weight (number-average, M_n) analysis was used to validate the MW determined through SEC and to evaluate the average number of ε-caprolactone units composing the macromonomer.

Nanoparticles Synthesis and Characterization. A glass three-necked flask was used to polymerize macromonomers through emulsion polymerization process as reported in Scheme 1. In particular, 1 g of emulsifier (SDS or Tween80) was dissolved in 100 mL of distilled water, and the solution was heated up to 50 °C in an oil bath and further purged by nitrogen for 30 min. After the injection of 5 g of macromonomer the initiator, 0.8 wt % potassium persulfate with respect to the monomer was added. The reaction was run for 3 h in order to ensure complete conversion of the macromonomer under a nitrogen stream of 5 mL/min. For semibatch reaction, the initiator was added before feeding the macromonomers into the reaction media at a fixed injection rate of 0.1 mL min^{-1}. Macromonomers with PCL chain length up to 4 are liquid and have been directly injected into the system. Higher MW macromonomers are solid at room temperature but liquid at the reaction temperature; thus, they were directly injected in the batch process before purging the system with nitrogen, while for semibatch reactions they were dissolved in 5 mL of dichloromethane and then injected into reaction media at a flow rate corresponding to 0.1 mL min^{-1} of macromonomer. As the dichloromethane boiling point is lower than the reaction temperature, it is completely removed by the nitrogen stream during polymerization.

Final particle size has been determined by light scattering (Malvern, Zetanano ZS); all data reported are an average value taken from two different measurements of the same sample. Finally, molecular weight of the polymer produced using SDS has been determined by SEC after particle precipitation by addition of a saturated sodium chloride solution and polymer extraction with THF.

Degradation Study. NPs produced through FRP were distributed into 10 mL glass vials and heated up to 50 ± 1 °C in a heating block. Samples were quenched at different times, and a qualitative analysis of the degradation process was performed through solution pH determination (Metrohm, 827 pHLab) and particle size measurements through dynamic light scattering (Malvern, Zetanano ZS).

3. RESULTS AND DISCUSSION

Macromonomer Production. As reported in the previous section, macromonomers with CL units between 1 and 10 were synthesized. All the produced macromonomers were analyzed by

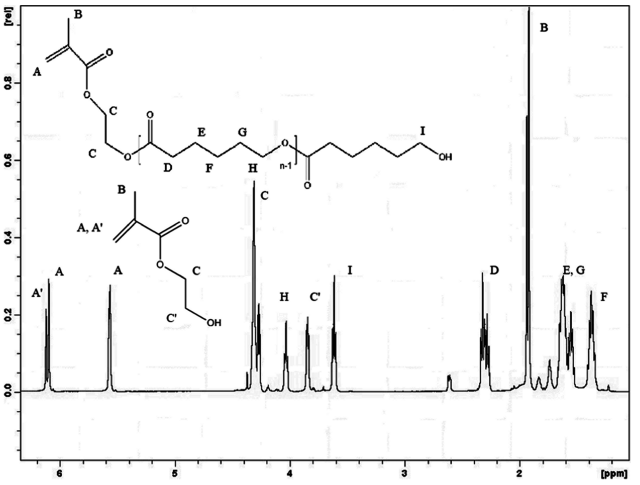

Figure 3. ^{1}H NMR spectra of HEMA-CL_1 macromonomer.

SEC. Since this technique is not reliable for oligomers as well as for very low MW polymer, SEC was combined with ^{1}H NMR measurement to determine the material MW and calculate the average CL units (*n*) added to HEMA molecule (Figure S1). A typical ^{1}H NMR spectrum of the synthesized macromonomers is reported in Figure 2.

Applying end-group analysis, it is possible to calculate the macromonomer MW as

$$M_n = M_{HEMA} + M_{\varepsilon\text{-caprolactone}}\left(\frac{H(\text{methylene proton signal})}{I(\alpha\text{ - methylene proton signal})} + 1\right) \quad (1)$$

where M_{HEMA} and $M_{\varepsilon\text{-caprolactone}}$ represent the molecular weight of HEMA and ε-caprolactone, respectively. With relation to Figure 2, *H* is representative of the total number of repeat ε-caprolactone units added, while *I* is the total number of terminal groups. As a result, the eq 1 term in parentheses, the ratio between the two terms to which is added the last unit (not considered in the *H* signal), represents *n*.

The NMR spectra also indicate that the macromonomers produced are of high purity, and the reactions were completed to high conversion, as seen from a close inspection of the CL and HEMA peaks in Figure 2, too small to be able to determine a final conversion, which is indeed higher than 98%. Moreover, the ratio of peak areas for the *A*, *C*, and *I* hydrogens in Figure 2 are in the expected 1:2:1 ratio. In addition, a control experiment with HEMA and $Sn(Oct)_2$ held at 130 °C in the absence of CL was conducted; it was found that HEMA does not thermally polymerize to any appreciable extent at reaction conditions.

However, the production of HEMA-CL_1 and HEMA-CL_2 macromonomers proceeded to lower HEMA conversions while ε-caprolactone remain very high; in these two cases the HEMA peak at 6.1 ppm, which represents hydrogen bonded to the HEMA vinyl end group, is split into two different peaks: *A* and *A*′, as shown in Figure 3. The *A* peak represents HEMA functionalized with CL units while *A*′ represents the free HEMA molecule. Considering the ratio of the two peak areas, it can be observed that HEMA conversion is between 60% and 80%. Likely, this lower conversion is due to the large amount of HEMA present in the system that cannot be fully activated by the catalyst. As a result, for these two macromonomers the final

dx.doi.org/10.1021/ma201955p |*Macromolecules* 2011, 44, 9205–9212

Table 1. Mark−Houwink Parameters for Poly(HEMA-*g*-CL_3), PHEMA, PCL, and PS

		Mark−Houwink parameters	
monomer	dn/dc (mL g^{-1})	K (dL g^{-1}) × 10^{-4}	a
poly(HEMA-*g*-CL_3)	0.0627	2.00	0.571
poly(HEMA)[30]	0.0556	2.39	0.537
PCL[31]		1.10	0.766
PS[30]	0.1800	1.14	0.716

mixture is a distribution of HEMA and HEMA functionalized molecules. In order to avoid results affected by the presence of unreacted HEMA, the two macromonomers were purified through precipitation. HEMA-CL_1 and HEMA-CL_2 were dissolved in absolute ethanol and then precipitated by adding distilled water. This procedure, repeated three times, leads to the HEMA removal, and the purified macromonomers were used for further polymerization.

As reported in the previous section, in order to obtain more reliable molecular weight from SEC analysis, poly(HEMA-*g*-CL_3) was selected to determine MH parameters. Various polymer samples were then analyzed leading to averaged parameters of $a = 0.571$ and $K = 2 \times 10^{-4}$ dL g^{-1}. As observed by the parameters summarized in Table 1, the poly(HEMA-*g*-CL_3) parameters are close to the poly(HEMA) ones while they are quite different from polystyrene (PS) and PCL.

Adopting the estimated MH parameters, a good agreement for M_n measurement between SEC and ^{1}H NMR was found especially for MW higher than 600, where GPC results are more reliable (the lower MW polystyrene standard used is 580 Da), as reported in Figure 4. Consequently, the universal calibration adopting HEMA-CL_3 was used for all the others macromonomers and polymer produced. All the pertinent data for the macromonomers produced are reported in Table 2. Except for the lower MW macromonomers, differences between the two analytical methods are less than 3%. Moreover, it is worth noticing that polydispersity data reported in Table 2 clearly demonstrate the controllable behavior of the macromonomer synthesis process.

Finally, the reproducibility of the process was also verified by synthesizing a number of samples at identical conditions. The resulting ^{1}H NMR analysis indicate good reproducibility of the macromonomers produced, with n between 2.2 and 2.4 for HEMA-CL_2 and between 3.3 and 3.5 for HEMA-CL_3.

Nanoparticles Production. NPs were produced from the synthesized macromonomers using the FRP batch procedure described in section 2, using SDS as surfactant. The properties of the poly(HEMA-*g*-CL_n) NPs produced are reported in Table 3. For each different macromonomer the final particle size and polydispersity index (PDI) measured at the end of the reaction are shown as well as polymer M_n measured by SEC. Figure 5 plots the average diameter of the NP as a function of macromonomer CL chain length.

As expected by adopting an emulsion polymerization process, small NPs with narrow particle size distribution are produced. The largest NPs are obtained with the macromonomer functionalized with 1 CL unit, as shown in Figure 5. The increase of the number of CL units, which is correlated to a decrease of the degree of polymerization, leads to a decrease in the diameter of the NPs, reaching a plateau value of 30 nm for CL units larger

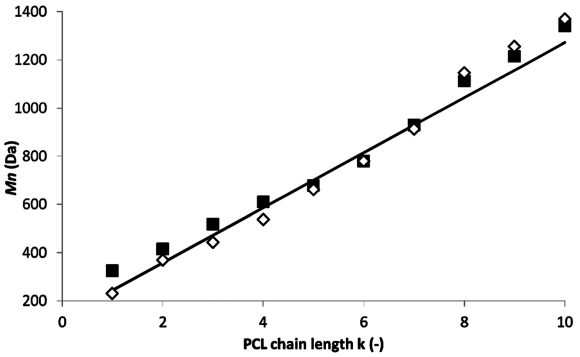

Figure 4. Macromonomer M_n vs CL chain length from (—) recipe, (■) ^{1}H NMR, and (◇) SEC.

Table 2. Characterization Data for All the Macromonomers Produced

recipe		^{1}H NMR		SEC	
k	M_n (Da)	n	M_n (Da)	M_n (Da)	M_w/M_n
1	244	1.7	324	230	1.20
2	358	2.5	415	369	1.39
3	473	3.4	518	443	1.42
4	587	4.2	609	538	1.29
5	701	4.8	678	661	1.29
6	815	5.8	780	780	1.38
7	929	7.0	929	913	1.31
8	1043	8.6	1112	1146	1.36
9	1157	9.5	1214	1256	1.37
10	1272	10.6	1340	1370	1.37

than 6. Finally, NPs produced with HEMA-CL_1 show a larger diameter in comparison to all the other NPs, most likely due to the more hydrophilic monomers that leads to the formation of NPs with a greater susceptibility to swelling.

The breadth of the particle size distribution, as well as the average value, is important for these materials. For macromonomers with low MW (up to 4 CL units) the final particle size distribution is quite narrow, as expected by adopting an emulsion FRP process. For macromonomers with CL units larger than 5, PDI of the particle size distribution increases from less than 0.06 to values between 0.1 and 0.2. Even if such values are indicative of a quite broad distribution, they are still acceptable since they remain lower than the PDI obtained through nanoprecipitation,[32] the conventional process used to obtain NPs made of biodegradable and biocompatible polyesters such as PCL.

As reported in the Introduction, for biomedical application the presence of SDS is not allowed. Thus, SDS has to be exchanged with a biocompatible emulsifier or the emulsion FRP reaction has to be directly performed with such a surfactant. Subsequently, NPs have been produced using Tween80 as a biocompatible steric emulsifier, as reported in the Experimental Section, with results summarized in Table 4. As it can be expected due to the lower efficiency of the steric surfactant compared to the anionic one for emulsion polymerization, all of these NPs have a final particle size higher than the ones produced using SDS. However, final particle size is still quite small, with average diameters all in

Table 3. Characteristics of NPs Produced through Emulsion Batch FRP Using SDS as Surfactant

CL chain length k	particle size (nm)	polydispersity index	particle size after ion exchange (nm)	polydispersity index after ion exchange	M_n (Da) SEC
1	55.2	0.095	66.8	0.268	4750
2	45.7	0.110	49.4	0.189	6065
3	39.2	0.036	51.2	0.075	6746
4	37.6	0.030	43.3	0.065	5296
5	39.0	0.125	40.3	0.204	5075
6	39.9	0.131	43.0	0.215	5186
7	27.9	0.222	32.8	0.310	4271
8	34.4	0.204	35.2	0.207	5570
9	29.0	0.174	30.4	0.229	5484
10	32.8	0.274	31.9	0.310	3895

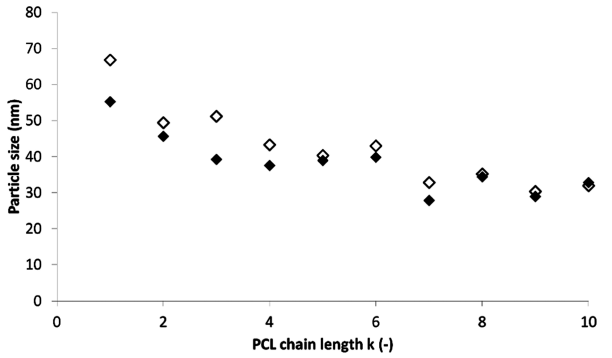

Figure 5. NPs sizes produced through batch emulsion polymerization: particle size vs CL chain length before (◆) and after (◇) treatment with ion exchange resins.

the range of 100 nm with the exception of the polymer produced using the HEMA-*g*-CL_1 macromonomer. The polydispersities of the particle size distribution follow the same behavior of the NPs produced with SDS, with an increase of the PDI observed with increasing macromonomer M_w, reaching values around 0.2 for larger macromonomers.

In order to obtain smaller diameter NPs stabilized with a biocompatible surfactant, the possibility of substituting SDS with Tween80 using ion exchange resins capable of selectively adsorbing the anionic surfactant has also been investigated. NPs suspension produced using SDS have been first mixed with 1 g of Tween80 and then stirred (2 h) together with an equal mass of ion-exchange resin in order to substitute the ionic emulsifier with the steric one. The resulting average particle size and PDI of the NPs are shown in Table 3. The surfactant substitution leads to NPs with almost the same dimensions as the original SDS-stabilized particles, with an increased PDI that is still acceptable for the final purposes.

So far, it has been shown that NPs down to 30 nm can be produced through batch processes. With the aim of further decreasing the average particle size, the use of a monomer starved semibatch emulsion polymerization process (MSSEP) has been investigated. In fact, it has been recently reported that under starved condition it is possible to produce very small NPs down to 15 nm.[33] NPs have been produced as reported in the Experimental Section (adopting DCM as solvent to feed higher MW macromonomers that are solid at room temperature), and the resulting NPs average diameters and PDI values are reported in Table 5.

Table 4. Characteristic of Nanoparticles Produced by Emulsion Polymerization Using Tween80

CL chain length k	particle size (nm)	PDI	CL chain length k	particle size (nm)	PDI
1	248.3	0.093	6	127.5	0.231
2	158.9	0.058	8	82.9	0.211
3	113.3	0.020	10	115.8	0.218
4	167.0	0.090			

Table 5. Nanoparticles Produced by Starved Emulsion Polymerization Using SDS

CL chain length k	particle size (nm)	PDI	CL chain length k	particle size (nm)	PDI
1	40.1	0.093	4	29.2	0.110
2	24.1	0.102	6	27.0	0.184
3	24.7	0.107	8	17.1	0.375

Comparing results reported in Tables 3 and 5 (graphically shown in Figure S5), it is seen that the MSSEP leads to the synthesis of NPs with much smaller diameter compared to the batch process, down to 17 nm for the NPs composed by poly(HEMA-*g*-CL_8). As was also observed for batch conditions, the macromonomer chain length affects the final achievable diameter using the MSSEP strategy. In particular, the diameter is decreased by increasing the hydrophobicity of the polymer (directly related to the CL chain length in the macromonomer), with the largest particles formed by polymerization of HEMA-CL_1. These NPs were synthesized using SDS as surfactant; this emulsifier can be substituted with Tween80 using the procedure described above to achieve a fully biocompatible system.

To summarize, adopting these new macromonomers in FRP processes makes it possible to synthesize NPs with well-controlled final particle size and narrow distribution by changing process parameters such as feeding condition, emulsifier type, and macromonomer chain length. The final NPs dimensions are ideal for biomedical uses such as invasive drug delivery. Moreover, it is worth mentioning the possibility to easily modify the macromonomer MW and thus tune the hydrophobicity of the resulting NPs to match that of the active drug component. Finally, since the degradation time is a function of the macromonomer MW as well as its hydrophobicity, it will be possible to

dx.doi.org/10.1021/ma201955p |*Macromolecules* 2011, 44, 9205–9212

Scheme 2. Degradation Mechanism of Poly(HEMA-*g*-CL$_k$) NPs

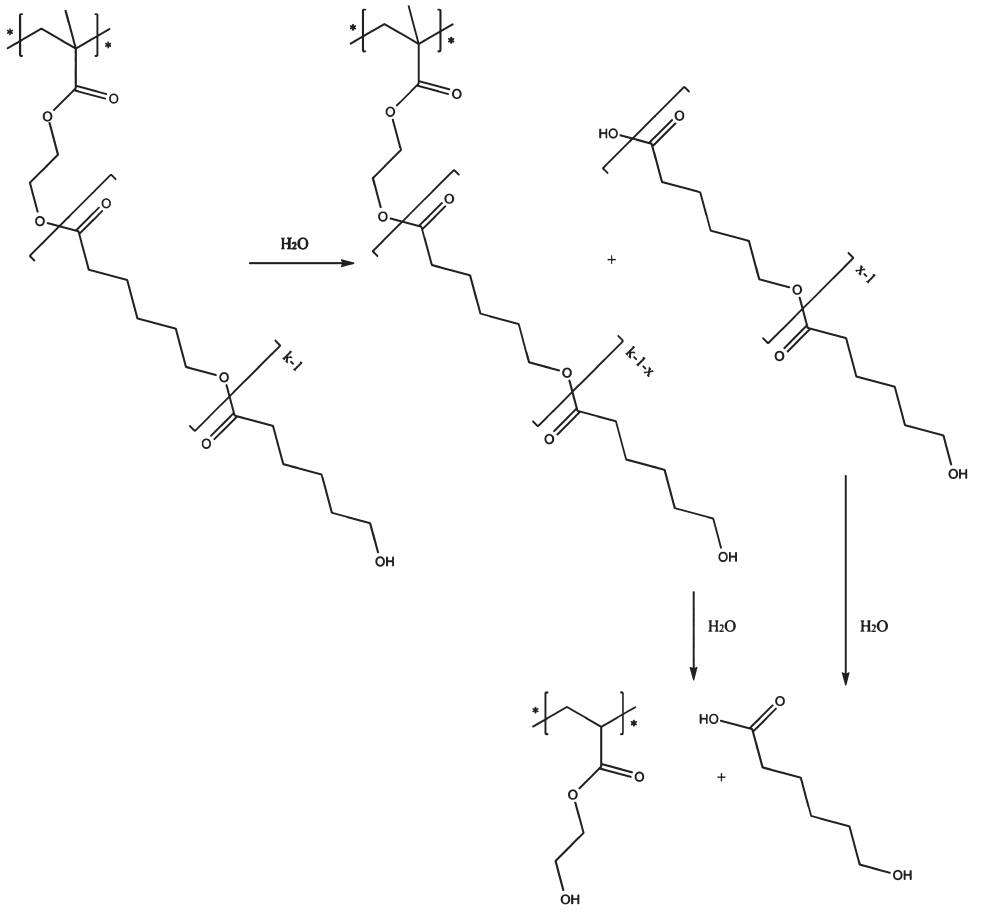

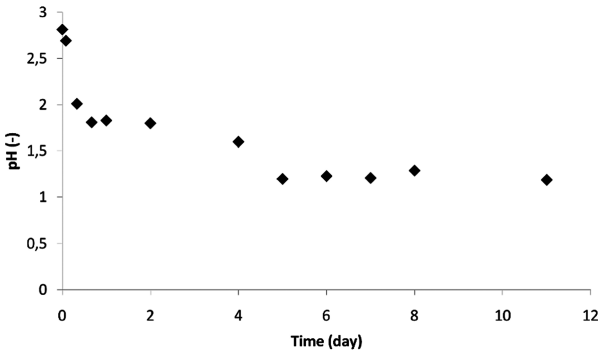

Figure 6. pH versus time during NPs degradations.

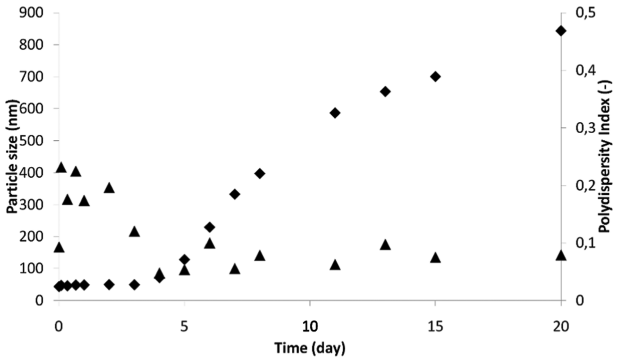

Figure 7. Particle size (♦) and polydispersity index (▲) versus time during NPs degradation.

easily tune also the degradation kinetics of these materials by changing the adopted macromonomer. In the next section the degradation behavior of these NPs is presented.

Degradation Study. As a final part of this work a preliminary study of the degradation behavior of these new materials was performed. Since the synthesis of these new macromonomers is mainly devoted to produce small biodegradable polymeric NPs, the degradation studies were focused on these final products. Thus, the study has been carried out on the produced NPs rather than studying the degradation of the macromonomer or bulk polymer. In order to prove the complete degradation of the NPs, the particle size evolution is followed as a function of the time up to complete disappearance. These measurements have been combined with a pH measurement in order to check the release of acidic species, as shown in Scheme 2.

NPs made by poly(HEMA-*g*-CL$_3$) produced in batch reaction using SDS as emulsifier were selected, with the characteristics of the starting materials reported in Table 3. The degradation study has been performed as reported in the Experimental Section. The starting pH of the NPs latex is 3 due to partial degradation of the macromonomer during the NPs synthesis. The pH evolution

during the polymerization has been monitored, and the final value is in agreement with a FRP process that adopts KPS and SDS, in which less than 2% of the macromonomer is hydrolyzed (Figure S4). The evolution of the particle size as well as the solution pH is reported in Figures 6 and 7. In order to avoid the addition of a chemical (usually a salt that interferes with the NPs stability) to buffer the solution, the degradation study has been performed without fixing the pH value. The pH measurements show an increase of acidity with time (Figure 6), explained by the release of acidic degradation products. In fact, since the degradation of the NPs proceed through the hydrolysis of ester bonds in the grafted PCL chain, 6-hydroxycaproic acid and its oligomers are released. The acidity increases until it reaches a plateau pH value of about 1.1. At the end of the degradation all of the oligomers released will be hydrolyzed into 6-hydroxycaproic acid, and the final composition of the system is characterized by the presence of this water-soluble acid and poly-HEMA as reported in Scheme 2.

Data reported in Figure 7 show the particle size evolution during the degradation period. The diameter of the NPs increases while the PDI remains constant during degradation (Figure S2). The enhancement of the NPs diameter cannot be ascribed to an aggregation process since the PDI remain constant but can be related to a swelling process. In fact, during the degradation time the polymer chains composing the NPs are continuously losing CL units and thus are becoming more and more hydrophilic. As a result, the polymer increases its affinity toward water that, through a swelling process, increases the NPs dimension. After a certain period (20 days for the studied NPs) water molecules that have diffused into the NPs completely hydrolyze the grafted PCL side units, leading to poly-HEMA chains which, being hydrophilic, are soluble in water. The complete degradation of the particles can be followed through LS measurement, with the end of the process characterized by the formation of a clear solution in which NPs can no longer be detected. All of the reported experimental results provide strong evidence of the degradability of these CL-based NPs. As a final part of this work the degradation of these NPs has been analyzed at room temperature for four different materials. Three different NPs batches were selected: poly(HEMA-*g*-CL_2) NPs obtained adopting SDS and Tween80 and poly(HEMA-*g*-CL_4) NPs with SDS. The degradation of NPs composed by poly(HEMA-*g*-CL_2) shows faster degradation for particles produced adopting Tween80 than the ones obtained with SDS. In fact, NPs with SDS (starting size of 50.8 nm) show a diameter of 67.8 nm after 3 months, 130 nm after 4 months, and are completely degraded after 6 months. At the same time, NPs with Tween80 (starting size of 130 nm) show a diameter increase up to 276 nm after 3 months and are completely degraded after 4 months. Even in these cases, the constant PDI obtained confirms the absence of any aggregation process. Finally, in order to prove the possibility to tune easily the degradation behavior of these novel NPs by changing the CL chain length, the degradation of poly(HEMA-*g*-CL_4) NPs using SDS has been performed. Starting from a diameter of 37.6 nm, these NPs show an increase of their size passing through 143 nm after 4 months and 254 nm after 6 months. These NPs are completely degradated after ~9 months. By increasing the branching length from two to four caprolactone units, the degradation time required is increased from 6 months to 9 months (Figure S3).

4. CONCLUSION

Short chain length poly(ε-caprolactone) macromonomers with varying CL length and functionalized with a vinyl end group have been synthesized and characterized by ^{1}H NMR spectroscopy and SEC. Mark−Houwink parameters for the HEMA-CL_3 macromonomer were determined, and the principle of universal calibration was applied to measure the MW of produced polymer and macromonomers. Subsequently, vinyl end groups have been polymerized through emulsion free radical polymerization in order to obtain NPs suitable for drug delivery applications. As a result, NPs characterized by a poly-HEMA backbone grafted with CL chains constituted by 1−10 CL units with tunable degradation behavior were obtained. These NPs have been synthesized in both batch and semibatch conditions and adopting different emulsifiers, namely SDS and Tween80. Adopting the steric Tween80 surfactant, NPs with diameter in the range 100−200 nm have been produced while, using SDS, the size has been easily tuned down to 17 nm. Moreover, the NPs degradation through hydrolysis has been demonstrated and qualitatively analyzed. NPs composed of poly(HEMA-*g*-CL_3) require less than 1 month to be completely degraded at 50 °C while the degradation time is equal to 4 months for poly(HEMA-*g*-CL_2) at room temperature. The capability to tune the degradation time by changing the macromonomer chain length has been shown. This new process is the first one proposed in the literature to produce in one pot nanoparticles made of biodegradable materials dispersed in waters (or biological media like for example PBS solution) without using any organic solvent. This peculiarity makes these novel nanoparticles attractive for biomedical applications.

■ ASSOCIATED CONTENT

Supporting Information. Figures S1−S5. This material is available free of charge via the Internet at http://pubs.acs.org.

■ AUTHOR INFORMATION

Corresponding Author
*E-mail: davide.moscatelli@polimi.it.

■ ACKNOWLEDGMENT

The authors acknowledge Dr. Marco Lattuada of ETH Zurich for fruitful discussions.

■ REFERENCES

(1) Holland, S. J.; Tighe, B. J.; Gould, P. L. Polymers for biodegradable medical devices. 1. The potential of polyesters as controlled macromolecular release systems. *J. Controlled Release* **1986**, *4* (3), 155–180.

(2) Laurencin, C. T.; Ulery, B. D.; Nair, L. S. Biomedical Applications of Biodegradable Polymers. *J. Polym. Sci., Part B: Polym. Phys.* **2011**, *49* (12), 832–864.

(3) Albertsson, A. C.; Varma, I. K. Recent developments in ring opening polymerization of lactones for biomedical applications. *Biomacromolecules* **2003**, *4* (6), 1466–1486.

(4) Storey, R. F.; Sherman, J. W. Kinetics and mechanism of the stannous octoate-catalyzed bulk polymerization of epsilon-caprolactone. *Macromolecules* **2002**, *35* (5), 1504–1512.

(5) Kweon, H.; Yoo, M. K.; Park, I. K.; Kim, T. H.; Lee, H. C.; Lee, H. S.; Oh, J. S.; Akaike, T.; Cho, C. S. A novel degradable

polycaprolactone networks for tissue engineering. *Biomaterials* **2003**, *24* (5), 801–808.

(6) Tomihata, K.; Suzuki, M.; Oka, T.; Ikada, Y. A new resorbable monofilament stature. *Polym. Degrad. Stab.* **1998**, *59* (1−3), 13–18.

(7) Klopp, L. S.; Simon, B. J.; Bush, J. M.; Enns, R. M.; Turner, A. S. Comparison of a caprolactone/lactide film (Mesofol) to two polylactide film products as a barrier to postoperative peridural adhesion in an ovine dorsal laminectomy model. *Spine* **2008**, *33* (14), 1518–1526.

(8) Hans, M. L.; Lowman, A. M. Biodegradable nanoparticles for drug delivery and targeting. *Curr. Opin. Solid State Mater. Sci.* **2002**, *6* (4), 319–327.

(9) Jia, X. Q.; Goldberg, M.; Langer, R. Nanostructured materials for applications in drug delivery and tissue engineering. *J. Biomater. Sci., Polym. Ed.* **2007**, *18* (3), 241–268.

(10) Brigger, I.; Dubernet, C.; Couvreur, P. Nanoparticles in cancer therapy and diagnosis. *Adv. Drug Delivery Rev.* **2002**, *54* (5), 631–651.

(11) Malin, M.; HiljanenVainio, M.; Karjalainen, T.; Seppala, J. Biodegradable lactone copolymers 0.2. Hydrolytic study of epsilon-caprolactone and lactide copolymers. *J. Appl. Polym. Sci.* **1996**, *59* (8), 1289–1298.

(12) Ye, W. P.; Du, F. S.; Jin, J. Y.; Yang, J. Y.; Xu, Y. In vitro degradation of poly(caprolactone), poly(lactide) and their block copolymers: Influence of composition, temperature and morphology. *React. Funct. Polym.* **1997**, *32* (2), 161–168.

(13) Soppimath, K. S.; Aminabhavi, T. M.; Kulkarni, A. R.; Rudzinski, W. E. Biodegradable polymeric nanoparticles as drug delivery devices. *J. Controlled Release* **2001**, *70* (1−2), 1–20.

(14) Chawla, J. S.; Amiji, M. M. Biodegradable poly(epsilon-caprolactone) nanoparticles for tumor-targeted delivery of tamoxifen. *Int. J. Pharm.* **2002**, *249* (1−2), 127–138.

(15) Damgé, C.; Socha, M.; Ubrich, N.; Maincent, P. Poly(ε-caprolactone)/eudragit nanoparticles for oral delivery of aspart-insulin in the treatment of diabetes. *J. Pharm. Sci.* **2010**, *99* (2), 879–889.

(16) Lince, F.; Marchisio, D. L.; Barresi, A. A. Strategies to control the particle size distribution of poly-epsilon-caprolactone nanoparticles for pharmaceutical applications. *J. Colloid Interface Sci.* **2008**, *322* (2), 505–515.

(17) Leroueil-Le Verger, M.; Fluckiger, L.; Kim, Y. I.; Hoffman, M.; Maincent, P. Preparation and characterization of nanoparticles containing an antihypertensive agent. *Eur. J. Pharm. Biopharm.* **1998**, *46* (2), 137–143.

(18) Molpeceres, J.; Guzman, M.; Aberturas, M. R.; Chacon, M.; Berges, L. Application of central composite designs to the preparation of polycaprolactone nanoparticles by solvent displacement. *J. Pharm. Sci.* **1996**, *85* (2), 206–213.

(19) Mei, L.; Zhang, Y.; Zheng, Y.; Tian, G.; Song, C.; Yang, D.; Chen, H.; Sun, H.; Tian, Y.; Liu, K.; Li, Z.; Huang, L. A Novel Docetaxel-Loaded Poly (ε-Caprolactone)/Pluronic F68 Nanoparticle Overcoming Multidrug Resistance for Breast Cancer Treatment. *Nanoscale Res. Lett.* **2009**, *4* (12), 1530–1539.

(20) Lamprecht, A.; Ubrich, N.; Perez, M. H.; Lehr, C. M.; Hoffman, M.; Maincent, P. Biodegradable monodispersed nanoparticles prepared by pressure homogenization-emulsification. *Int. J. Pharm.* **1999**, *184* (1), 97–105.

(21) Yuan, W.; Yuan, J.; Zhou, L.; Wu, S.; Hong, X. Fe3O4@poly(2-hydroxyethyl methacrylate)-graft-poly(ε-caprolactone) magnetic nanoparticles with branched brush polymeric shell. *Polymer* **2010**, *51* (12), 2540–2547.

(22) Moscatelli, D.; Lattuada, M.; Morbidelli, M.; Yu, Y. *Method for Making Customized Nanoparticle, Nanoparticles and Use Thereof.* EU patent 11004059.9-2112, May 17, 2011.

(23) Stjerndahl, A.; Wistrand, A. F.; Albertsson, A.-C. Industrial Utilization of Tin-Initiated Resorbable Polymers: Synthesis on a Large Scale with a Low Amount of Initiator Residue. *Biomacromolecules* **2007**, *8* (3), 937–940.

(24) Moravek, S. J.; Storey, R. F. Copolymers of rac-Lactide and ε -Caprolactone: Conventional Copolymerization vs. Macroinitiator Copolymerization. *J. Macromol. Sci., Part A* **2009**, *46* (4), 339–345.

(25) Morbidelli, M.; Yu, Y. C.; Storti, G. Ring-Opening Polymerization of L,L-Lactide: Kinetic and Modeling Study. *Macromolecules* **2009**, *42* (21), 8187–8197.

(26) Odjan, G. *Principles of Polymerization*; J. Wiley & Sons: New York, 2004.

(27) Chern, C. S. Emulsion polymerization mechanisms and kinetics. *Prog. Polym. Sci.* **2006**, *31* (5), 443–486.

(28) Sajjadi, S.; Yianneskis, M. Semibatch emulsion polymerization of methyl methacrylate with a neat monomer feed. *Polym. React. Eng.* **2003**, *11* (4), 715–736.

(29) von Burkersroda, F.; Schedl, L.; Gopferich, A. Why degradable polymers undergo surface erosion or bulk erosion. *Biomaterials* **2002**, *23* (21), 4221–4231.

(30) Moscatelli, D.; Dossi, M.; Liang, K.; Hutchinson, R. A. Investigation of Free-Radical Copolymerization Propagation Kinetics of Vinyl Acetate and Methyl Methacrylate. *J. Phys. Chem. B* **2010**, *114* (12), 4213–4222.

(31) Schindler, A.; Hibionada, M.; Pitt, C. *J. Polym. Sci., Polym. Chem. Ed.* **1982**, 20.

(32) Nagesh, K.; Shanta, D.; M, V. P.; Q, L. L.; Rohit, K.; J, L. S.; Robert, L.; C, F. O. Engineering of self-assembled nanoparticle platform for precisely controlled combination drug therapy. *Proc. Natl. Acad. Sci. U. S. A.* **2010**, *17* (42), 17939–17944.

(33) He, G.; Pan, Q.; Rempel, G. L. Synthesis of Poly(methyl methacrylate) Nanosize Particles by Differential Microemulsion Polymerization. *Macromol. Rapid Commun.* **2003**, *24* (9), 585–588.